Explorations of combined nonsolvent and thermally induced phase separation (N-TIPS) method for fabricating novel PVDF hollow fiber membranes using mixed diluents

Jie Zhao[a,b], Jeng Yi Chong[a], Lei Shi[a], Rong Wang*[,a,b]

[a]Singapore Membrane Technology Centre, Nanyang Environment and Water Research Institute, Nanyang Technological University, 1 Cleantech Loop, Singapore 637141, Singapore

[b]School of Civil and Environmental Engineering, Nanyang Technological University, 50 Nanyang Avenue, Singapore 639798, Singapore

*Corresponding author at: School of Civil and Environmental Engineering, Nanyang Technological University, Singapore 639798, Singapore. Email: rwang@ntu.edu.sg

Abstract

The combination of nonsolvent and thermally induced phase separation (N-TIPS) method has shown promising ability in harvesting the features from the nonsolvent induced phase separation (NIPS) and thermally induced phase separation (TIPS) processes for developing membranes with a tailorable surface pore structure. However, previous approaches have been subjected to either the formation of macrovoids or dense layer due to the dominant NIPS effect, or required sophisticated instruments and operation skills. In this work, a facile attempt was carried out to fabricate novel polyvinylidene fluoride (PVDF) hollow fiber membranes with tunable surface pore structure while maintaining the narrow pore size distribution and mechanical strength. A modified N-TIPS method was developed by using mixed diluents: dimethyl phthalate (DMP) as a water-immiscible poor solvent for TIPS process, and triethyl phosphate (TEP) as a water-miscible neutral solvent to bridge the TIPS and NIPS processes. To further control the membrane formation especially near the membrane surface, an amphiphilic additive Pluronic F127 was also added as a potential pore-former and surface hydrophilicity modifier. PVDF hollow fiber membranes with a highly porous structure and a narrow pore size distribution were successfully synthesized by using TEP and Pluronic F127 in the N-TIPS process. The mechanism of N-TIPS process was thoroughly discussed. The water permeability of the membrane increased significantly from 389 ± 30 to 922 ± 36 L $m^{-2}h^{-1}bar^{-1}$, with overall porosity improved from 50 ± 2.2 to 69 ± 2.9 %, and a mean pore size of ~0.18 μm. The membranes produced by N-TIPS method also exhibited a good tensile strength ranging from 5.6 ± 0.1 to 6.5 ± 0.2 MPa, showing a great potential for a broad range of water applications after further modifications. Besides, the formation of piezoelectric β-phase crystals of the PVDF membrane was observed when the mixed diluent was used, which

sheds light on the possible applications of resultant membranes in electrochemical separation process.

***Keywords*:** Polyvinylidene fluoride; Hollow fiber membrane; Combined nonsolvent and thermally induced phase separation; Pluronic F127.

1. Introduction

Membrane-based separation processes have been widely utilized in the clean water and energy production [1], biopharmaceutical [2], food and agricultural [3] industries which are essential to human life. The polymeric membranes used in these processes can be fabricated via several approaches and the phase inversion method is currently the mainstream technique used for most polymeric membrane productions [4]. Among the different phase inversion methods, two techniques are frequently used: thermally induced phase separation (TIPS) and nonsolvent induced phase separation (NIPS) [5]. The TIPS method is normally employed to fabricate membranes from thermoplastics such as poly(methyl methacrylate) (PMMA) [6], polypropylene (PP) [7] and polyvinylidene fluoride (PVDF) [3]. The phase separation occurs due to the temperature gradient when the polymer solution (hot front) is in contact with the coagulant (cold front). Subsequently, the pore structure is formed and fixed along with the crystallization of polymer. The membranes prepared via the TIPS method usually possess a narrow pore size distribution and high mechanical strength [8]. Notably, as the TIPS method is composed of only two components (polymer and diluent), membranes fabricated by the TIPS method are inherently reproducible and less prone to defects than other phase inversion methods [9]. However, the membrane surface properties such as pore size and hydrophilicity cannot be effectively controlled using pore-formers with different functions in the same way as the NIPS method [10]. This can be attributed to the weak mass transfer in the conventional TIPS process as a result of the low mutual affinity between the commonly used TIPS diluents and the nonsolvent (usually water). Owing to this disadvantage, the surface pore size of TIPS membranes can hardly be tuned without significantly changing the bulk membrane structure, which limits the application of the TIPS technique [11]. In comparison, the NIPS method involves three major components: polymer, solvent, and

nonsolvent. The membrane formation starts at the interface between the polymer solution and the nonsolvent, which is driven by the solvent-nonsolvent exchange [12]. The NIPS technique can expediently adjust the pore size and other surface characteristics of membranes with the help of additives, as shown in many previous studies [13, 14]. Nevertheless, the NIPS membranes are frequently subjected to the macrovoids or defects formed during the solvent-nonsolvent exchange. The mass transfer has been found to be around two order slower than the heat transfer in the solution [15], providing less evenly distributed driving force than that in the TIPS process. In addition, the instability of polymer/solvent dope at the solvent-nonsolvent interface also contributes to the difficulty in controlling the phase inversion process. As a result, membranes produced by the NIPS process often exhibit a wider pore size distribution and weaker mechanical properties than the TIPS membranes [16].

Researchers have been trying to bridge the gap between TIPS and NIPS by using different approaches as listed in Table 1. For the same chemical, the terms “diluent” (in TIPS) and “solvent” (in NIPS) are used interchangeably in this paper to emphasize its function in different processes. The study reported by Matsuyama and co-workers in 2002 has been recognized as the first attempt of the combined NIPS and TIPS (N-TIPS) method [15]. During the fabrication of PMMA membranes, they proposed to modify the conventional TIPS method by using cyclohexanol as the diluent, which possesses a high affinity with the nonsolvent. The diluent induced the NIPS process by facilitating the solvent-nonsolvent exchange at the dope-coagulant interface. Similar attempts of using a water-soluble diluent (TIPS solvent) have been made in the past decades (approach 1 in Table 1) [5, 15, 17-20]. However, the sole use of water-soluble diluent might steer the phase inversion to a NIPS-dominated N-TIPS process. The membranes produced often exhibit two types of morphology which are normally undesired: (a) a dense layer with

nearly no pores due to fast out-diffusion of diluents [15, 17, 18]; or (b) a bulk structure intruded by finger-like macrovoids from the surface layer caused by the rapid exchange as a result of a large concentration gradient between the water-soluble diluent and water [8, 20]. The dense skin layer can drastically reduce the permeability, while the macrovoids in the bulk structure are critically regarded as fragile parts which can significantly curtail the lifetime of hollow fiber membranes [4, 16]. On the other hand, some researchers chose another direction by performing modified NIPS process at an elevated temperature (approach 2 in Table 1) [18, 21-25]. They used common NIPS solvents such as N,N-dimethylacetamide (DMAc) and N-methyl-2-pyrrolidone (NMP), which are water-soluble strong solvents for PVDF at the room temperature, and obtained the membrane structures similar to the approach 1. Membranes prepared through this method inherit drawbacks mostly from the NIPS membranes, which include broad pore size distribution and macrovoids [21, 22]. Moreover, such dope system can only be operated at a relatively low temperature owing to the low boiling point of the common NIPS solvents [22]. The reduced temperature gradient may not allow sufficient time for the crystallization of polymer during membrane formation, which could compromise the membrane mechanical properties [26]. Recently, researchers in this field have been trying to co-extrude the TIPS dope mixture with a NIPS coating solution [27] or a solvent [11, 28] on the outer channel using a triple-orifice spinneret (approach 3 in Table 1). However, this approach requires demanding coordination between the dope mixtures and coating solution during the spinning. Membranes prepared are also subjected to possible delamination and irregular surface structure due to asynchronous curing process of the dual layer [29].

As illustrated in Fig. 1, we summarized the solvents/diluents commonly used in the N-TIPS process into four different categories based on their solubility with polymer and water. The solvents which can dissolve the polymer at the room temperature are defined as

good solvents [9]. The good solvents, which are water-soluble, are often used in the NIPS process [30-32]. For instance, NMP and DMAc are common NIPS solvents for PVDF [33]. On the other hand, those water-insoluble poor solvents are normally used as diluents in the TIPS process. For PVDF, such diluents include dimethyl phthalate (DMP), dibutyl phthalate (DBP), diethyl phthalate (DEP), acetyl tributyl citrate (ATBC), etc. [3]. Among various solvents, we found triethyl phosphate (TEP) is a special one that cannot be fitted into this figure [34]. TEP is a water-soluble solvent with a high boiling point (215 °C) and is able to completely dissolve PVDF only at a moderately high temperature (80 °C for PVDF at 20 wt%) [35]. Thus, it can be considered as a neutral solvent for PVDF. It is able to induce both TIPS and NIPS processes under appropriate conditions [17]. It has also been listed as one of the promising non-toxic alternatives to the conventional toxic solvents, such as DMAc, DBP, DEP, etc [36-38]. However, the membrane formation was found to be strongly hindered by the gelation induced possibly at high TEP concentration [35].

Herein, we proposed a modified N-TIPS approach using mixed diluents, which contain a water-insoluble poor solvent and a water-soluble neutral solvent. This simple method is expected to allow us to tune the surface pore structure of membranes effectively without forming mechanically weak macrovoids, and to scale up membrane fabrication easily. Specifically, the water immiscible plasticizer, DMP, was used as the main diluent for PVDF since the hollow fiber membranes prepared from the PVDF/DMP dope mixtures exhibited an outstanding mechanical strength in our previous work [39]. TEP was used at a low concentration together with DMP for PVDF fabrication in an effort to control the solvent-nonsolvent concentration gradient and to avoid the occurrence of gelation. To further increase the membrane surface porosity, amphiphilic copolymer Pluronic F127 was used as an additive. F127 has shown excellent surface-modifying and pore-forming abilities [40], and its effects on N-TIPS PVDF membranes were also studied. This research

aims at providing a facile approach for developing robust hollow fiber membranes with a tunable macrovoid-free surface pore structure, followed by studying the fundamental phenomena in the membrane formation during the N-TIPS process.

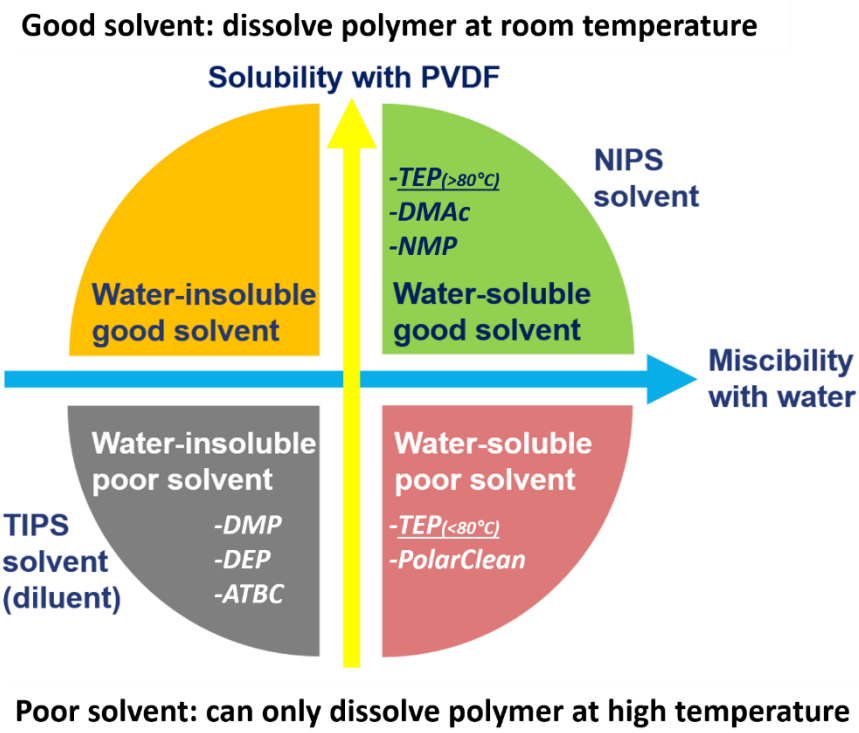

Fig. 1. Four types of solvents categorized according to their solubility with polymer (PVDF) and water

Table 1. Some published reports on the combined TIPS and NIPS (N-TIPS) method

Year	First author	Polymer	Additive	Solvent/diluent	Geometry	Ref.
Approach 1: Modified TIPS by using a water-soluble poor solvent (TIPS solvent) as diluent						
2002	Matsuyama, H.	PMMA	\	Cyclohexanol	FS	[15]
2015	Wu, L.	PVDF	\	DCAC	FS	[18]
2015	Xiao, T.	PVDF	\	CPL	FS	[20]
2015	Hassankiadeh, N. T.	PVDF	PVP, PMMA, glycerol	PolarClean	HF	[19]
2016	Jung, J. T.	PVDF	Pluronic F127, LiCl, glycerol, PVP	PolarClean	FS	[5]
Approach 2: High-temperature NIPS by using NIPS solvent or by adding a water-soluble good solvent into diluent						
2008	Li, X.	PVDF	\	DBP/DMAc	FS	[22]
2013	Qin, A	PVDF	PEG	GBL/DMAc	HF	[24]
2014	Wu, L.	PVDF/PES-C	\	DPC/DMAc	FS	[21]
2014	Liu, J	PVDF	\	TEP/GBL/glycerol/sulfolane/DMAc	FS/HF	[25]
2015	Xu, H.	PVDF	PFSA	NMP	FS	[23]
Approach 3: Co-extrusion by extruding a NIPS coating solution or a solvent on the outer layer using a triple-orifice spinneret						
2015	Lee, J.	PVDF	PVP, glycerol, LiCl	GBL/NMP	HF	[27]
2018	Fang, C.	PVDF	\	GTA, DEP, ATBC, glycerol, PEG 400, 1,3- butanediol, GBL, TEP, NMP	HF	[28]
2018	Jung, J. T.	PVDF	\	DBP, ATBC, NMP, PolarClean	HF	[11]

*Abbreviations (order of appearance): PMMA, poly(methyl methacrylate); PES-C, phenolphthalein polyethersulfone; PVP, poly(vinylpyrrolidone); PFSA, perfluorosulfonic acid; DCAC, diethylene glycol monoethyl ether acetate; CPL, ε-Caprolactam; PolarClean, methyl-5-(dimethylamino)-2-methyl-5-oxopentanoate; DBP, dibutyl phthalate; DMAc, N,N-dimethylacetamide; DPC, diphenyl carbonate; NMP, N-methyl-2-pyrrolidone; GBL, γ-butyrolactone; GTA, glycerol triacetate; DEP, diethyl phthalate, ATBC, acetyl tributyl citrate; PEG, polyethylene glycol; TEP, triethyl phosphate; FS, flat sheet; HF, hollow fiber.

2. Experimental

2.1 Materials

Polyvinylidene fluoride (PVDF Solef® 1015, M_w = 570,000 – 600,000, Solvay, Belgium) was purchased for the fabrication of hollow fiber membranes. Dimethyl phthalate (DMP, Merck KGaA, Germany) was used as the main diluent and bore fluid. Triethyl phosphate (TEP, Merck KGaA, Germany) was used as the second diluent. Pluronic® F127 (abbreviated as F127 in the following paragraphs, M_w = 12,600, PEO_{100}–PPO_{65}–PEO_{100}, Sigma Aldrich, Singapore) was used as an additive in hollow fiber fabrication. Ethanol (Merck KGaA, Germany) and n-hexane (Merck KGaA, Germany) were used successively in the post-treatment for resultant membranes. Bovine serum albumin (BSA, M_w = 67,000, Sigma-Aldrich) was used as a model protein foulant. Milli-Q ultra-pure water was used as the de-ionized (DI) water for all experiments. All the reagents were used as received.

2.2 Phase diagram determination

The StarFish Workstation (Heidolph Instruments, Germany) was used to prepare the samples of dope mixtures at 220 °C. The method for cloud point (T_{cloud}) measurement of the polymer-diluent system was adapted from a previous study [41]. After cooling, the solidified dope mixtures were sliced into small dices of specimens (diameter about 0.5 cm) and then inserted into two cover slips. Upon mounted on a hot stage (Linkam THMS600, UK), the specimen was heated up to 200 °C and then cooled down to 40 °C. The cooling rate was fixed at 10 °C min^{-1}. The T_{cloud} was determined visually at the first sight of liquid droplets under an optical microscope (Nikon Eclipse 50i, Japan). The gelation curve was obtained by identifying the points at which the homogeneous solutions began to transform into turbid gels [35, 42].

A differential scanning calorimeter (DSC, Q20, TA Instruments, USA) was used to analyze the thermal behavior of dope mixtures in a dry nitrogen atmosphere. About 5 mg of the dope mixture was tightly encapsulated into an aluminum pan (Tzero pan and Tzero hermetic lid, TA Instruments, USA) for each specimen measurement. Prior to the melting tests, the thermal history of the sample was erased by a rapid ramp up to 200 °C at a rate of 40 °C min^{-1}. Upon equilibrating at 200 °C for 2 min, the crystallization curve was attained by cooling to 40 °C at a rate of 10 °C min^{-1} [9]. The onset temperature of the exothermic peak was then defined as the dynamic crystallization temperature (T_c) (the initial point of crystallization) in the cooling process [43]. The phase diagrams were obtained by plotting the cloud points (if any) and the crystallization curve jointly. Subsequently, the melting behavior of dope mixtures was also investigated at a heating rate of 10 °C min^{-1}.

2.3 Preparation of hollow fiber membranes

PVDF hollow fiber membranes were developed using a set of spinning apparatus [39]. PVDF, DMP, TEP and F127 particles in predetermined concentrations as described in Table 2 were fed to the dope tank. The dope mixture was then mixed and heated to 220 °C for 2 h in a dry nitrogen (with purity of 99.9995%) atmosphere in order to obtain a homogeneous solution. The gas bubbles in the dope mixture were released during a 1-h standstill without mixing at 220 °C. During the spinning process, the dope mixture was dispensed into a spinneret, which was kept 200 °C, using a gear pump under the pressure of nitrogen gas at about 1 bar. The bore fluid (bore fluid) was pumped at various flow rates into the spinneret at room temperature using a syringe pump (Teledyne ISCO Inc., Model 1000D). Tap water was used as the external coagulant. The dope mixture was extruded from the spinneret together with the bore fluid along a short air gap prior to entering the quenching bath. Upon contact between the hot dope mixture and cold coagulants, the inception of phase inversion occurred at both outer (shell) and inner (lumen) interface, leading to the formation of hollow fiber membrane. The nascent hollow fiber membranes were immersed into DI water for 24 h to achieve sufficient solidification. In an effort to

extract the residual diluents, the post-treatment was then conducted by soaking the membranes in ethanol for 24 h and then immersing into n-hexane for 3 h. The hollow fiber membranes were dried in air at room temperature prior to characterization [10]. The samples with TEP weight fractions at 0, 5, 10 wt% were designated as T0, T5 and T10, accordingly. On top of T5, the samples with F127 weight fractions at 1 and 3 wt% were designated as T5F1 and T5F3. The corresponding characteristics of resultant membranes are summarized in Table 2. The spinning parameters are listed in Table 3.

Table 2. Dope compositions used for the membrane preparation

Code[a]	PVDF (wt%)	DMP (wt%)	TEP (wt%)	Pluronic F127 (wt%)
T0		70	0	0
T5		65	5	0
T10	30	60	10	0
T5F1		64	5	1
T5F3		62	5	3

Notes:
[a)] Bore fluid composition (wt%): DMP (100).

Table 3. Spinning parameters for hollow fiber membranes

Extrusion rate (g min^{-1})	5.3
Extrusion temperature (°C)	200
Bore fluid flow rate (mL min^{-1})	2.0
Bore fluid temperature (°C)[a]	25
Quenching temperature (°C)	30
Air gap (cm)	1
OD/ID of spinneret (mm)	1.84/0.92

Notes:
[a)] The temperature before entering the spinneret.

2.4 Characterization of hollow fiber membranes

The dimension of resultant hollow fiber membranes was measured by a digital microscope (VHX-500F, Keyence, USA). A scanning electron microscope (SEM, Zeiss EVO 50, Carl Zeiss AG, Germany) was used to examine the morphology of membranes. By fracturing the frozen hollow fibers in the liquid nitrogen, the samples for cross-sectional observation were prepared. The samples were then coated with a conductive gold layer using a gold sputter coater (Emitech SC7620, Quorum Technologies, UK) before the observation [10].

The pore size distribution of membranes was measured by a capillary flow porometer (CFP 1500A, Porous Material. Inc., USA). To ensure the fully wetting of pores, the membranes were immersed in a wetting liquid (Galwick, with a low surface tension of 15.9 dynes cm^{-1}) overnight. The wetting liquid saturated in the wetted pores was then displaced by the compressed dry nitrogen gas. The calculation of pore size distribution, bubble point pore size and mean pore size were carried out by the software equipped with the porometer [13]. The overall porosity of membranes was determined based on the gravimetric method by applying the following equation [40]:

$$\varepsilon = 1 - \frac{\rho_m}{\rho_p} = 1 - \frac{M / V_m}{\rho_p} \quad (1)$$

where ε is the membrane overall porosity; ρ_m is the membrane density; M is the weight of dry membrane; V_m is the volume of membrane which can be calculated from its inner/outer diameter (ID/OD); ρ_m is the specific gravity of PVDF which has a value of 1.78 g cm^{-3} as provided in the Solvay product information [44]. To reduce the uncertainty that might result from the deviation of inner diameter/outer diameter (ID/OD) along the length of fibers, a mean value of three times of measurement was recorded [44]. The surface porosity of membranes was obtained by analyzing the SEM images using ImageJ. The procedures can be found in a previous study [5].

The analysis of crystalline properties of PVDF membranes was conducted using a DSC. Dried hollow fibers in 4 – 5 mg were sealed in an aluminum pan. The test was performed following the same cool-heat procedure as described in Section 2.2. The degree of crystallinity was calculated based on the following equation [45]:

$$\chi_c = \frac{\Delta H}{\Delta H_m} \times 100\% \tag{2}$$

where χ_c is the degree of crystallinity (%); ΔH and ΔH_m represent the fusion enthalpy (melting enthalpy) of the membrane and PVDF with 100% crystallinity, respectively; The value of ΔH_m is 104.5 J g^{-1} [40].

The crystal structure of PVDF in prepared membranes was examined through the wide angle X-ray diffraction (WAXD) in a Bruker D8-Advance diffractometer (Cu Ka radiation, 40 kV and 40 mA). The scanning velocity was set to 4° min^{-1} with the scanning angle ranging from 5 to 50. The crystal size of PVDF in the membranes was estimated by Scherrer's equation [46, 47]:

$$D = K\lambda / \beta \cos\theta_d \tag{3}$$

where D is the estimated diameter of the crystals (nm); K is the Scherrer's constant (K=0.89); λ is the wavelength of the incident x-rays (nm), which is 0.154 in this study; β is the peak width at half height (rad); θ_d is the diffraction angle (rad).

The surface chemistry properties of prepared membranes were analyzed by the attenuated total reflectance Fourier transform infrared spectroscopy (ATR-FTIR, IR Prestige-21, Shimadzu, Japan). To increase the surface area for scanning, hollow fibers were cut in a short length and compressed

prior to the test. The IR spectra were obtained by analyzing the surface of dried membranes by 45 scans at a resolution of 4 cm^{-1} [40].

The dynamic contact angle of prepared membranes was measured using a tensiometer (DCAT11 Dataphysics, Germany) based on the Wilhelmy method [14]. A piece of dried fiber in a length of 1 – 1.5 cm was firmly attached onto a hanging arm of an electronic balance. A cycle of measurement was then carried out by dipping the sample into DI water followed by lifting at an advancing/receding speed of 0.2 mm min^{-1} with an immersion depth of 5 – 10 mm. The change in weight was recorded continuously by the electronic balance. For each specimen, three cycles were measured. The membrane sample was in a dry state before the immersion at the first cycle. The value of contact angle obtained at the second cycle was lower than the first one because some of the pores at surface had been probably filled with water. The contact angle of the second advancing cycle was selected in this study to reflect the hydrophobicity of membranes since it is believed to better represent the real situation in practical applications [14]. Each run was repeated 3 – 5 times to ensure the reproducibility.

The mechanical properties of prepared membranes were analyzed using a tensile meter (Zwick/Roell Z 0.5 kN Universal Testing Machine, Germany). The specimen of hollow fibers at a length of 55 mm was inserted into the testing clamp and then pulled longitudinally at an elongation rate of 50 mm min^{-1} at room temperature. The corresponding mechanical properties containing the tensile modulus, tensile strength and elongation were subsequently determined with the aid of built-in software [31].

2.5 Filtration test of hollow fiber membranes

Test modules of membranes were assembled for the performance test in the cross-flow configuration. For each module, 4 – 6 fibers were inserted into a PP tube. The tube was then sealed on both ends using an epoxy adhesive to achieve an effective length of 16.3 cm. The filtration set-up was

described in a previous study [48]. Prior to the test, the membranes were compacted by circulating the DI water through the shell side of hollow fiber membranes for 30 min under a constant pressure of 1 bar. The pure water permeability (PWP, J_0, L $m^{-2}h^{-1}bar^{-1}$) was then calculated by [48]:

$$PWP = \frac{V}{tA\Delta P} \tag{4}$$

where V is the permeate volume (L) measured per determined time, t (h); A is the filtration area of the membrane (m^2); ΔP is the pressure difference between the feed and the permeate sides of the membrane (bar).

3. Results and discussion

3.1 Thermodynamic properties of PVDF/DMP/TEP ternary system

Determining the thermodynamic properties of the polymer-diluent mixture is important for the understanding of N-TIPS membrane formation mechanism. The interactions between polymer and the mixed diluents are discussed in two scenarios: (a) between PVDF and individual diluent, and (b) between PVDF and the diluent mixture. The mutual affinity of a polymer and a solvent/diluent can be estimated by the Hansen's solubility parameter (δ_t) which comprises of three dimensional components: polar (δ_p), dispersion force (δ_d), and hydrogen bonding (δ_h) [49]. In scenario (a), the individual relative affinity of PVDF with DMP and TEP can be examined by the following equation [13]:

$$\Delta\delta_{ps} = ((\delta_{ps} - \delta_{pp})^2 + (\delta_{ds} - \delta_{dp})^2 + (\delta_{hs} - \delta_{hp})^2)^{1/2} \tag{5}$$

where p and s represent the polymer and the solvent, respectively. Normally, a smaller value indicates a better interaction between the polymer and the solvent.

The solubility parameters are listed in Table 4. It can be seen that the value of $\Delta\delta_{ps}$ for PVDF and DMP is greater than that of PVDF and TEP, which suggests that the interaction of PVDF polymer chains with DMP is weaker than that with TEP. TEP also possesses a stronger affinity with PVDF than some of the common NIPS solvents such as DMAc and NMP, and PVDF can be completely dissolved in TEP at a moderately high temperature (80 °C for PVDF at 20 wt%) [35]. In addition, TEP has a high boiling point and miscibility with water. Such features render TEP a promising solvent to induce the low-temperature TIPS and high-temperature NIPS [17]. The versatility of TEP was expected to play a key role in inducing the N-TIPS process.

Table 4. Solubility parameters of PVDF and some common solvents

Chemicals	δ_d	δ_p	δ_h	δ_t	$\Delta\delta_{ps}$	Boiling point	Miscibility with H_2O	Ref.
			$(MPa)^{1/2}$			(°C)		
PVDF	17.2	12.5	9.2	23.2	-	-	Low	[20]
DMP	18.6	10.8	4.9	21.9	4.8	283.0	Low	[50]
TEP	16.8	11.5	9.2	22.3	1.1	215.0	High	[16]
DMAc	16.8	11.5	10.2	22.7	1.5	165.0	High	[16]
NMP	18.4	12.3	7.2	22.9	2.3	202.0	High	[16]

We also examined the interaction between PVDF and the mixture of DMP and TEP in scenario (b) based upon the Flory-Huggins solution theory [51, 52]. The estimation of the interaction parameter (χ^*) can be expressed by the difference of the solubility parameters between polymer and the diluent in the following equation [53, 54]:

$$\chi^* = \frac{V_m}{RT}((\delta_{d1} - \delta_{d2})^2 + (\delta_{p1} - \delta_{p1})^2 + (\delta_{h1} - \delta_{h1})^2) \quad (6)$$

where V_m is a reference volume which equivalents to the molar volume of the specific repeating unit size of the polymer; R is the gas constant; T is the temperature; for δ_d, δ_p and δ_h, 1 and 2 denote the polymer and diluent, respectively. Assuming that V_m is identical for all systems, the interaction between PVDF and diluents for dope mixtures at a certain temperature and polymer concentration could be expressed by molar excess free energy of mixing (ΔG^E) [54]:

$$\Delta G^E = (\delta_{d1} - \delta_{d2})^2 + (\delta_{p1} - \delta_{p1})^2 + (\delta_{h1} - \delta_{h1})^2 \quad (7)$$

where small values of χ^* or ΔG^E indicates better interaction between polymer and the diluent.

As listed in Table 5, five combinations of polymer and diluent mixtures were used to assess the interaction between PVDF and the mixtures of DMP and TEP. The value of each solubility parameter for the diluent mixtures was calculated as follows [41, 54]:

$$\delta_i = \delta_{i1}\varphi_1 + \delta_{i2}\varphi_2 \quad (8)$$

where φ is the volume fraction of the diluent, 1 and 2 refer to DMP and TEP, respectively; i represents d, p and h. By solving Eq. (7) and (8), ΔG^E can be determined accordingly. The value of ΔG^E decreased with increasing the weight fraction of TEP in the diluent mixture, which indicates that the increase of TEP in diluent mixtures enhanced the interaction between polymer and diluent mixture.

Table 5. Solubility parameters of diluent mixtures containing 30 wt% PVDF

Diluent mixture (TEP/DMP, wt%/wt%)	δ_d	δ_p	δ_h	ΔG^E
		$(MPa)^{1/2}$		$(J\ m^{-3})$
0/70	18.6	10.8	4.9	23.3
5/65	18.5	10.9	5.2	20.3
10/60	18.3	10.9	5.5	17.5
15/55	18.2	11.0	5.8	14.8
20/50	18.1	11.0	6.1	12.5

In order to determine suitable membrane synthesis conditions, the phase diagrams of the PVDF/DMP/TEP ternary system were determined, as shown in

Fig. 2. The illustration of a ternary system in TIPS process is usually difficult and error-prone due to its complexity which involves four dimensions, i.e., three concentrations (1 polymer, 2 diluents) and temperature [41]. In this study, we projected these four dimensions onto two two-dimensional figures to help describe the interrelations among them clearly. Firstly, to discuss the effect of mixed diluents on the system, the depiction was based on variations of TEP ratios where the PVDF concentrations were fixed at 30 wt%, as shown in

Fig. 2(a). The crystallization temperature decreased significantly with increasing TEP content in the diluent mixture. It agrees with the finding that the affinity of the diluent mixture with PVDF can be enhanced by adding TEP as a second diluent as shown in Table 5. However, gelation took place when the concentration of TEP was higher than 40 wt%. It suggests that a relatively low weight fraction of TEP in the system is preferred to avoid the possible formation of a dense gel layer due to the gelation [42, 55]. Thus, we selected 5 and 10 wt% TEP in this study. When TEP fractions were fixed at 0, 5 and 10 wt%, we obtained the crystallization and cloud point curves by varying the weight fractions of PVDF as shown in

Fig. 2(b - d). The monotectic points of the systems with 0, 5, 10 wt% TEP additions appeared to be at about 29, 27, 26 wt% of PVDF, respectively. In this study, we selected 30 wt% as the polymer concentration to ensure that there was adequate viscosity for continuous processing based on our previous study [39]. At the selected polymer concentration, the TIPS process is more likely to develop along the route of solid-liquid (S-L) phase separation instead of the liquid-liquid (L-L) phase separation

[26, 39]. In addition, it also shows that 200 °C is high enough to guarantee the homogeneity of dope solutions at all polymer concentrations.

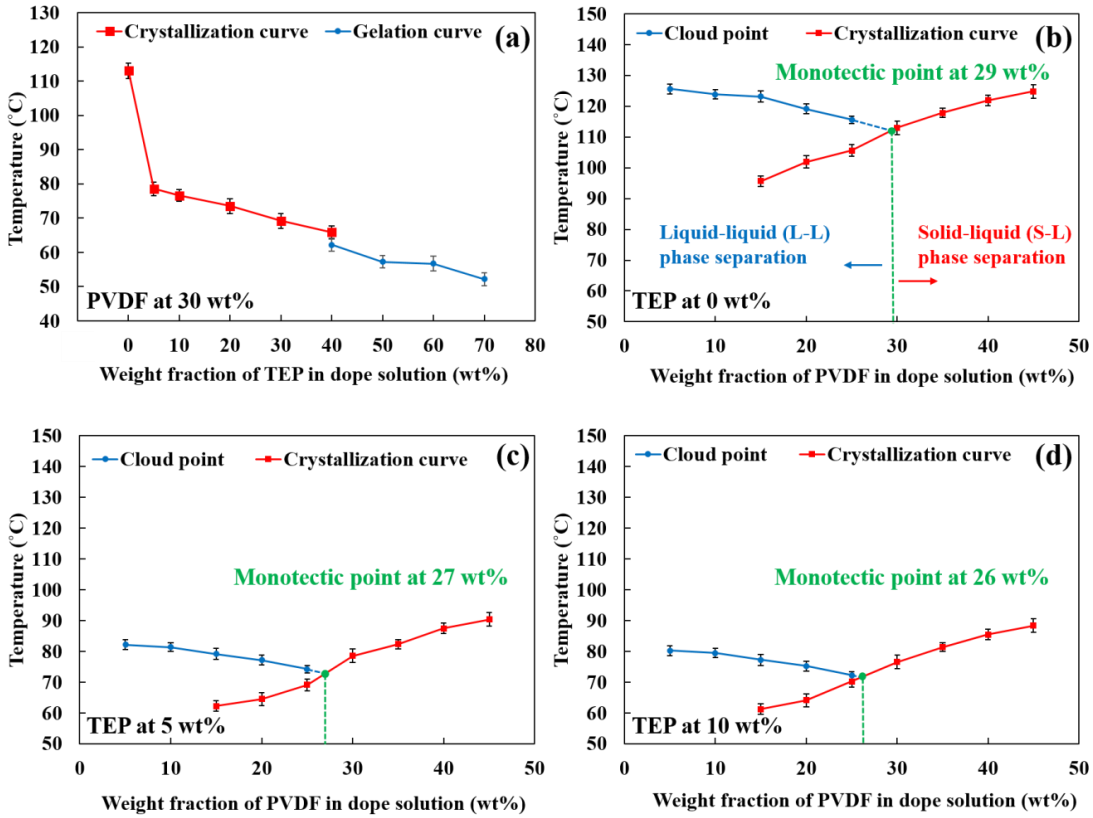

Fig. 2. Phase diagrams for PVDF/DMP/TEP system based on different weight fractions of (a) TEP, where the PVDF concentration is fixed at 30 wt% and an increase in TEP weight fraction was compensated by a decrease in DMP weight fraction; (b-d) PVDF, where TEP concentrations are fixed at 0, 5, 10 wt%, respectively

3.2 Morphological properties of membranes and possible mechanism for the formation of membrane structure

In the study, the addition of the water-miscible TEP and F127 was expected to induce the NIPS process near the membrane surface along with the TIPS process throughout the bulk of membrane structure. Fig. 3 displays the SEM images of the cross-sections and the surfaces of the as-spun hollow

fibers from different PVDF/DMP/TEP dope systems. In the cross-sectional images as shown in Fig. 3(a), the general spherulite-like structures can be found in all membranes. However, the morphologies vary from one to another in terms of the shape, size and density of the spherulites and cavities among them. For the virgin membrane (T0), a non-typical spherulitic structure was obtained, which comprised of loosely packed spherulites with large cavities in between. The boundaries of spherulites could hardly be spotted, while some regions appeared similar to the bicontinuous structure. Meanwhile, a relatively dense layer was observed at the outer surface. A relatively smooth outer surface was formed in the virgin membrane (T0) by tightly connected spherical crystalline structure, suggesting a low outer surface porosity. With 5 wt% of TEP added (T5), stronger impingements can be found among the spherulites with larger sizes and more discernable peripheries. The spherulites became smaller and more compact when the fraction of TEP was augmented to 10 wt% (T10). The morphology turned into a rugged surface with protuberant spherulites and ravines in between. The protruding structure then grew thicker but smoother on the surface with clear canyons at the bottom with a further addition of TEP (T10). However, the borders of the spherulites gradually disappeared with the addition of F127 from 1 to 3 wt% (T5F1 and T5F3). The plausible bicontinuous structure dominated the bulk cross-sectional morphology of T5F3, leaving only a minor portion of spherulitic-like structure. From the cross-sectional view, the outer surfaces of membranes with F127 addition appeared to be more porous than those without F127. A porous sponge-like surface layer in a shape of valley can be seen in T5F3. In regard to the inner surface as presented in Fig. 3(c), without TEP addition (T0), the membranes exhibited moderate pore sizes among others. The membranes with TEP added (T5 and T10) exhibited slightly fewer pores on the inner surface than the virgin one (T0). However, it can be seen that a more porous structure was obtained with the addition of F127 (T5F1 to T5F3).

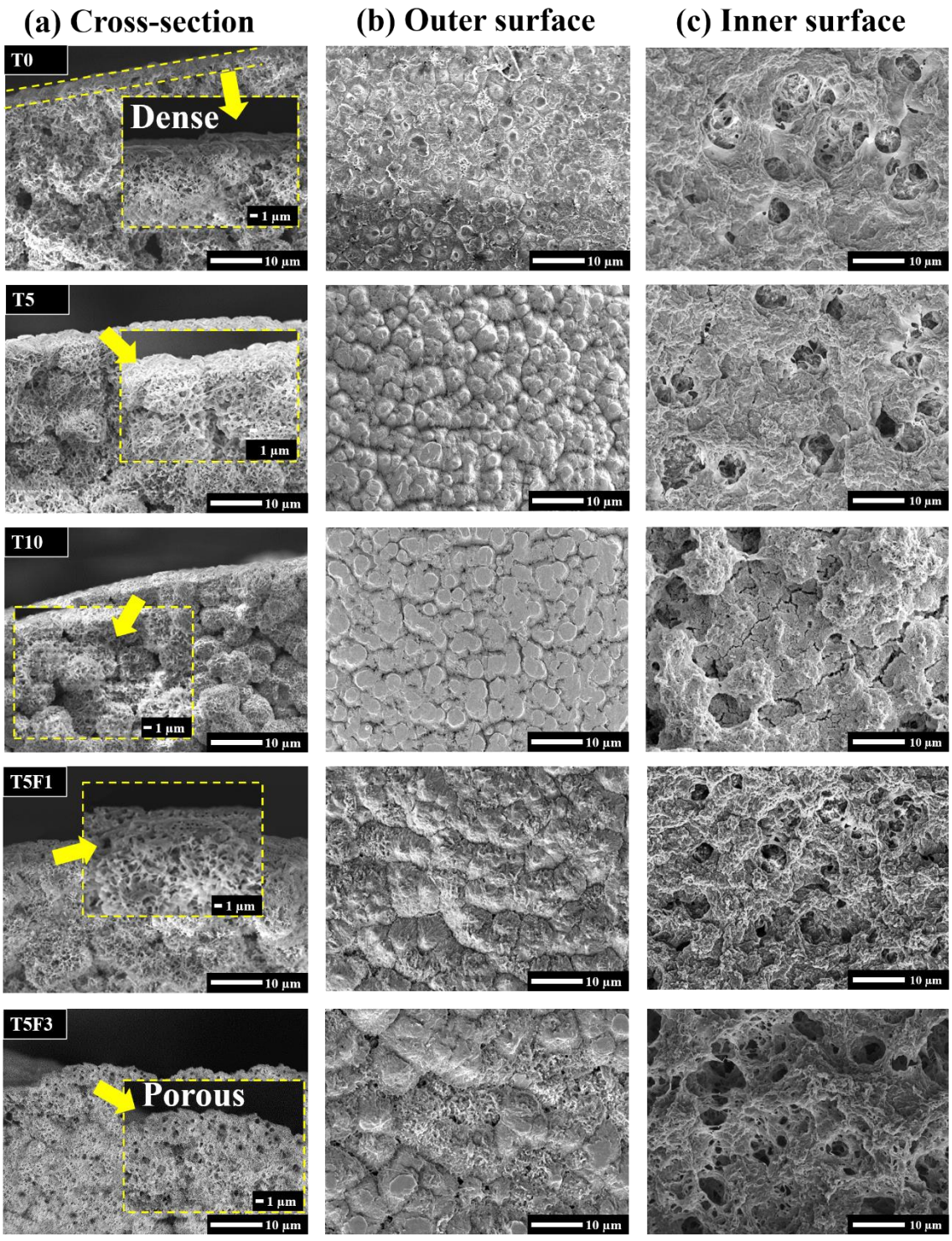

Fig. 3. SEM images of hollow fiber membranes obtained with different mixed diluents and Pluronic F127 fractions: (a) cross-section near outer surface (2,000X) with enlarged inserts (5,000X); (b) outer surface (2,000X); (c) inner surface (2,000X).

In order to provide clear explanations for the membrane morphology obtained, we proposed a conceptual schematic drawing to visualize our understanding of the membrane formation mechanism, as shown in Fig. 4. When DMP was used as a single diluent, the presence of spherulitic structures indicates that the S-L phase separation in the TIPS process (C1 in Fig. 4) was dominant in the formation of the bulk structure of membranes. The indistinct boundaries of spherulites suggest a weak impingement of spherulites during the coarsening and perfection of crystallization [41]. Apart from the S-L phase separation, the L-L phase separation (C2) might also have taken place in certain areas where the local PVDF concentration was below the monotectic point (29 wt%, close to 30 wt% as used) as bicontinuous-like structure was found in some regions. Besides that, a dense layer was also observed near the membrane outer surface when only DMP was used as the diluent. This could be ascribed to the low affinity between DMP and the nonsolvent (water), resulting nearly no inflow of nonsolvent. In this scenario, the composition near the outer surface might shift to the polymer-rich region possibly due to the outflow of diluents during the solidification of polymer matrix. Consequently, a relatively dense layer with small pores was formed owing to the high polymer concentration generated by the outflow of diluent (O1).

When mixed diluents containing TEP as a bridging agent (diluent in TIPS, solvent in NIPS) were used, the formation of spherulites in smaller sizes and a higher density could be attributed to the enhanced polymer-diluent interaction as discussed in Section 3.1. An enhanced interaction could postpone the phase separation and subsequent crystallization, allowing less time for spherulite growth [26]. In addition, the mutual affinity between the diluent mixture and nonsolvent (water) was also enhanced with the presence of TEP. This allowed the N-TIPS process to happen, and an increase inflow of nonsolvent produced was likely to rebalance the ratio of outflow to inflow. Though the NIPS process might be limited with the small amount of TEP, it still helped open up the pore structure near the membrane surface. The effect of NIPS became more significant with the addition of F127 in the

polymer dope solution especially at concentration 3 wt% where a porous sponge-like surface layer can be seen clearly from the SEM image. At a moderate quenching temperature, solvent-nonsolvent (TEP/water) exchange may happen at a relatively low rate (O2). The formation of sponge-like structure provides strong evidence for the occurrence of NIPS processes at the outer surface but can also be ascribed to the pore-forming effect of the amphiphilic F127 as it could participate in the pore formation upon contact with the water inflow [40]. This study did not reveal the case when a high rate of solvent-nonsolvent exchange was achieved. It is possible that the typical macrovoid structure could be obtained if sufficient amount of TEP was added into the external quenching tank to increase the exchange rate at the outer surface of membranes [42, 55]. Matsuyama and co-workers have demonstrated that the macrovoid structure can be observed from a PMMA/cyclohexanol system, which is likely to involve the exchange between cyclohexanol and water (nonsolvent) [15]. Similar morphology with finger-like macrovoid structure has also been reported by Jung and co-workers using water-soluble PolarClean as the diluent for PVDF [5] (O3).

Different from the situation on the shell side, the bore fluid used on the lumen side was DMP. The contact between the polymer solution and the bore fluid took place in the stainless spinneret which was kept at 200 °C. Thus, the temperature gradient on the lumen side was lower than that on the shell side, contributing to a dampened heat transfer rate and a slower crystallization. Without TEP addition (T0), the polymer concentration near the interface was hardly changed, leading to moderate pore sizes as compared with others (I1). As the out diffusion of TEP occurred at the interface, the polymer concentration was increased and thus the structure became less porous (I2). When F127 was added from 1 to 3 wt%, the inner pore structure was probably opened up by the aggregated instable F127 particles which might diffused out along with the diluent outflow[56]. Above all, the pore formation at the inner surface could be mainly influenced by the diluent diffusion driven by the concentration gradient of TEP during the TIPS process.

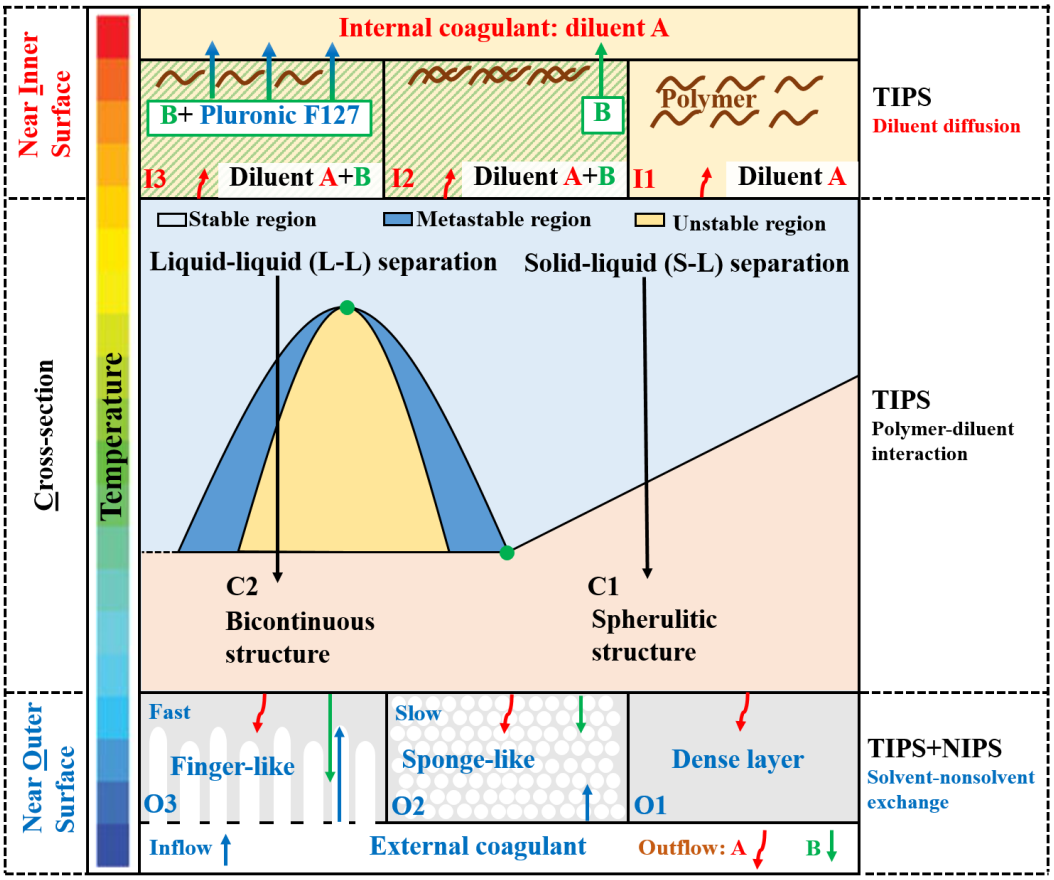

Fig. 4. Proposed conceptual illustration of N-TIPS process

3.3 Pore size distribution and water permeability of hollow fiber membranes

Fig. 5(a) depicts the pore size and pore size distribution curves of the produced PVDF membranes. The results of porosity are presented in Fig. 5(b). It can be seen that both the mean and the maximum pore sizes of the membranes increased with the addition of TEP (T5 and T10) and F127 (T5F1 and T5F3) as compared to the virgin membrane (T0). Meanwhile, the curves of the pore size distribution maintained a similar shape even with the increase in pore size and porosity as shown in Fig. 5(a) and 5(b). From the SEM images shown in Fig. 3, we can find that the pores on the inner surface are far larger than those on the outer surface. Thus, the mass transfer resistance is expected to be mostly determined by the pores in the bulk structure or on the outer surface. The formation of these pores can be mainly explained by two major factors. Firstly, with the addition of TEP, smaller spherulites in a

higher density were formed due to enhanced polymer-diluent interaction during the TIPS process, which can reduce the pore size. Similar reductions in the pore size due to a higher density of spherulites were reported in our previous study [39]. Secondly, the pores were opened up in a large amount as a result of solvent-nonsolvent (TEP/water) exchange, which can be supported by the increase in the pore size and porosity as shown in Fig. 5(b). It should be pointed out that the pore size and porosity of T10 appeared to be smaller than that of T5. This could be ascribed to the stronger impact of the increase in the polymer-diluent interaction over the solvent-nonsolvent (TEP/water) exchange, which probably fixed the pore structure before the NIPS process came into effect. The effect of these two factors was likely to be rebalanced with the addition of F127. Dual functions might be provided by F127 in this process, i.e., (a) hindering the polymer-diluent interaction; (b) participating in the pore formation due to its affinity with the external coagulant (water) at the outer surface or aggregation-led mobility at the inner surface [57]. Therefore, the pore size and porosity could be tuned by inducing N-TIPS effect using the combination of mixed diluents and F127. The overall porosity of membranes was improved from 50 ± 2 to 69 ± 3 % without widening the pore size distribution. From Fig. 5(b) and Fig. 6, it can be found that the PWP results are strongly correlated with the pore size and porosity of tested membranes. The water permeability of membranes was increased from 389 ± 30.3 (T0) to 1060 ± 29 (T5F3) L $m^{-2}h^{-1}bar^{-1}$. When TEP and F127 was added to induce the N-TIPS effect, the enlarged pore size and porosity significantly contributed to the enhancement in PWP.

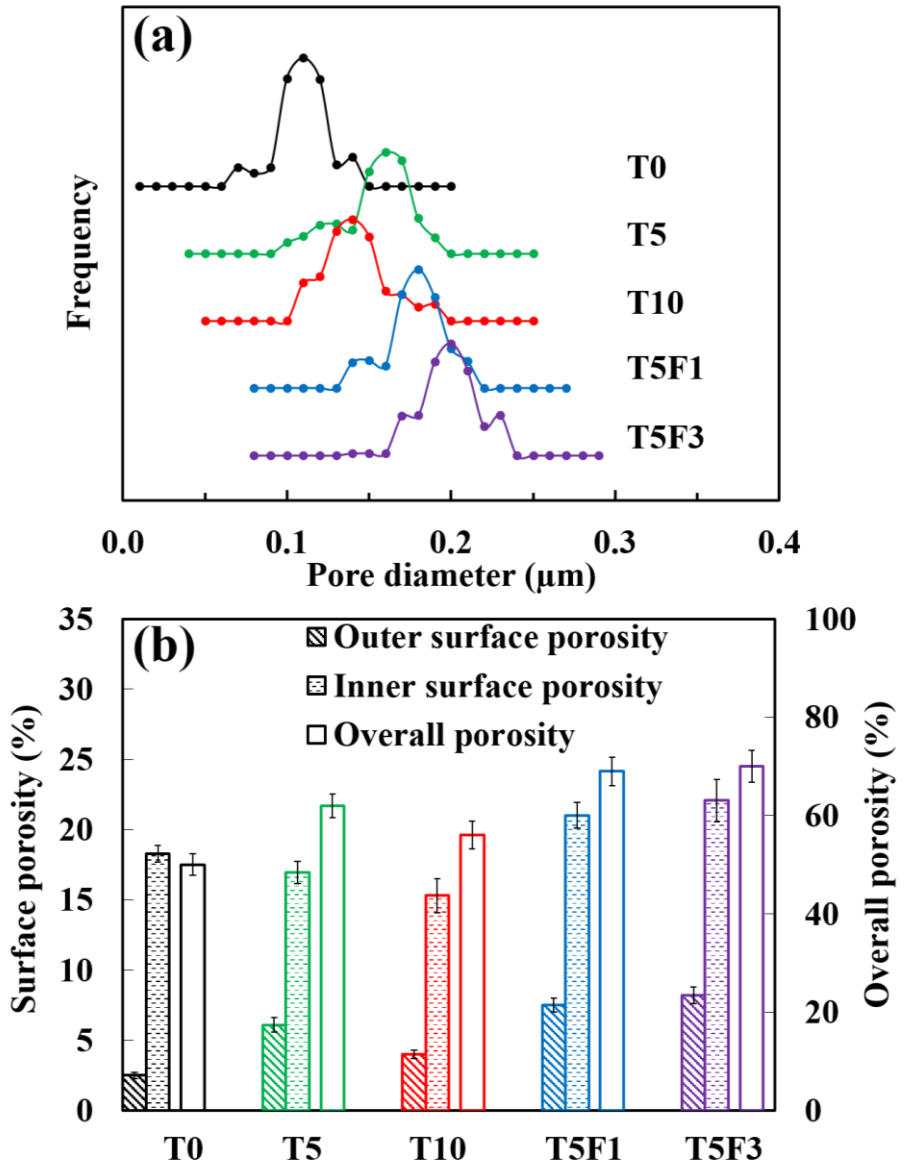

Fig. 5. Pore size distribution (a), and porosity (b) of membranes obtained with different mixed diluents and Pluronic F127 fractions

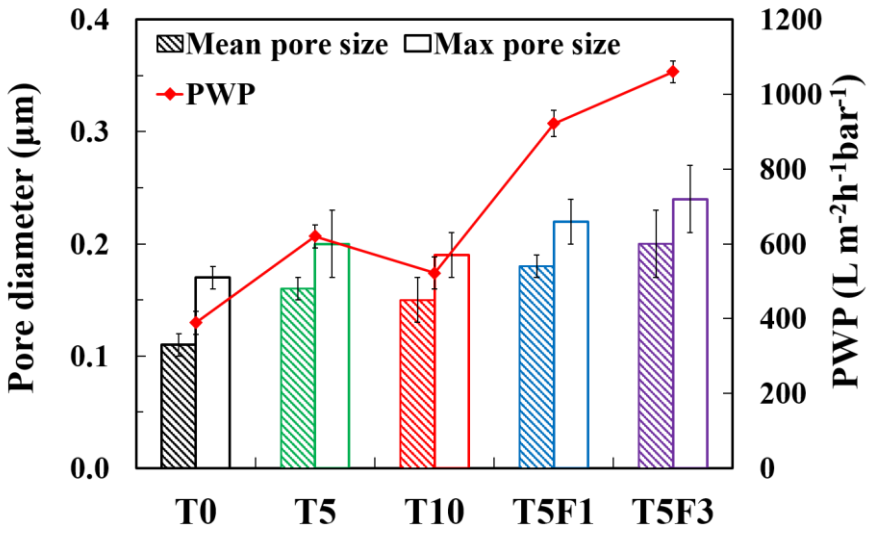

Fig. 6. Pure water permeability and corresponding pore size of membranes obtained with different mixed diluents and Pluronic F127 fractions.

3.4 Hydrophobicity of hollow fiber membranes

The surface hydrophobicity can normally be indicated by the water contact angle and the surface roughness of membranes as presented in Table 6 and Fig. 7. It can be seen that the water contact angle increased from 96 ± 6 to 103 ± 5° with the gradual addition of TEP, indicating the formation of a more hydrophobic outer surface. This is probably due to the hydrophobic nature of PVDF and the increased surface roughness. As suggested by SEM images in Fig. 3, the embossment of spherulitic structure on the outer surface became more evident with protruding spherulites when mixed diluents were used. Still, the contact angle of T5F1 dropped to 89 ± 3° with 1% of F127 addition, but then increased to 105 ± 6° at 3 wt% F127 fraction (T5F3). With the addition of F127, the exposed spherulites were similar to the lotus structure, which increased the surface roughness and could consequently enhance the hydrophobicity [58]. On the other hand, the incorporation of the amphiphilic block copolymer may have also changed the surface property. F127 comprises of hydrophilic polyethylene oxide (PEO) and hydrophobic polypropylene oxide (PPO) units. During the N-TIPS process, the hydrophobic PPO units

can adsorb onto the PVDF matrix, anchoring itself in the membranes. The hydrophilic PEO units can thus protruding exteriorly, equipping the membrane surface with better hydrophilicity [59]. The decrease in contact angle with 1 wt% of F127 addition can be ascribed to the exposed hydrophilic units on the outer surface. However, for membranes with a higher concentration of F127, the stability was found to be subjected to the possible aggregation behavior [40, 60, 61]. This could be responsible for the increase in contact angle of T5F3 as the surface roughness might dominantly affect the hydrophobicity if the F127 was washed out. The presence of F127 will be further analyzed based on the FTIR results in the next section.

Table 6. Surface properties of membranes obtained with different mixed diluents and Pluronic F127 fractions

Membrane code	Dynamic contact angle (°)	R_a of outer surface (nm)
T0	96 ± 6	49.4 ± 0.5
T5	101 ± 4	68.5 ± 0.6
T10	103 ± 5	53.2 ± 0.9
T5F1	89 ± 3	62.5 ± 0.7
T5F3	105 ± 6	75.0 ± 1.2

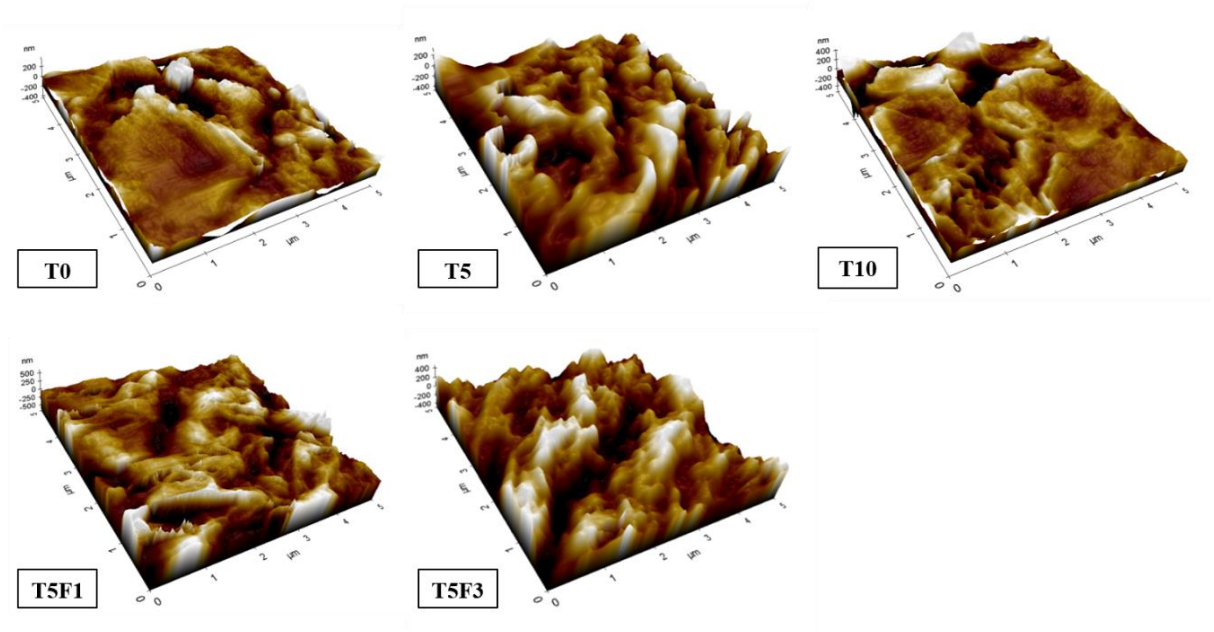

Fig. 7. AFM images (3D) of the outer surface of membranes obtained with different mixed diluents and Pluronic F127 fractions

3.5 Crystalline properties of hollow fiber membranes and presence of additives in membranes

In previous sections, it was found that the TIPS effect mainly contributed to the formation of the bulk structure by controlling the phase inversion and the subsequent crystallization of PVDF. The intrinsic properties of the semi-crystalline PVDF are greatly dependent on its crystal structure, which can consequently affect the durability and other important properties of the membranes. Therefore, it is necessary to investigate the crystalline characteristics of prepared membranes to further understand the effects of mixed diluents and F127 on the TIPS process. As shown in Fig. 8(a), the peak crystallization temperature of the dope mixtures decreased drastically after introducing TEP into the mixture (T0 to T5), and then continued to drop slightly with a further increase in the TEP fraction from 5 wt% to 10 wt% (T5 to T10). The result was also presented in the phase diagram in

Fig. 2(a). However, the crystallization temperature bounced back when the F127 was added to the mixture (T5 to T5F1 and T5F3), which suggests that the PVDF-diluent interaction was probably weakened.

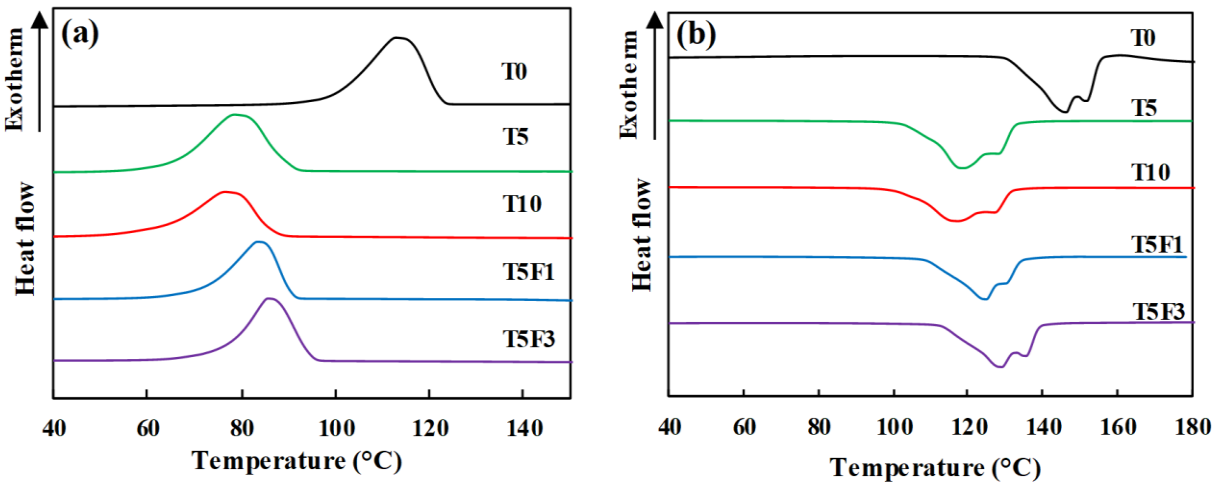

Fig. 8. Crystallization and thermal behaviors of dope mixtures with different mixed diluents fractions: (a) crystallization curves; (b) melting curves

The melting curves of dope mixtures are shown in Fig. 8 (b). All the curves exhibit the phenomenon of "double melting endotherms", which involves a low melting endotherm and a high melting endotherm [41]. It can be seen that the high melting endotherm was dampened with the addition of TEP from 5 wt% to 10 wt% (T0 to T5 and T10). However, the peak of the low melting endotherm grew back into a similar shape when F127 was added into the dope mixtures (T5 to T5F1 and T5F3). The occurrence of "double melting endotherms" can normally be attributed to: (a) the presence of polymorphism [62], (b) a secondary crystallization during the heating process [41]. As shown in Fig. 9(a), the peaks at $2\theta = 17.66°$, 18.30° and 19.90° in the WAXD patterns for both virgin and TEP-added membranes relate to the diffractions in planes (100), (020), and (110), respectively, which indicates the presence of α-phase crystals of PVDF [3]. However, the β-phase crystals of PVDF were only found in the TEP-added membranes as confirmed by the peaks at $2\theta = 20.26°$, 41.22° (in planes (200) and

(201)) [3, 63]. The addition of TEP was shown to be responsible for the formation of β-phase in the surface layer of PVDF membranes previously [64]. It was possible that the mass transfer induced by TEP at the interface might have resulted in a high polymer concentration near the surface. That could facilitate the oriented packing of CH_2-CH_2 dipoles and the conformation of consequential trans-trans-trans (TTT) which are correlated to the formation of β-phase [65]. Possessing a good piezoelectricity, the β-phase is normally preferred in the fabrication of membranes for electrochemical purposes such as the polymer electrolyte in the lithium-ion batteries. The antifouling properties of PVDF membrane can also be enhanced by applying AC signals to generate the vibration [66].

Owing to the absence of β-phase crystals in the virgin membrane, the prevalent appearance of "double melting endotherms" could not be fully explained by the existence of polymorphism. Previous studies have revealed the correlation of the spherulitic structure with the secondary crystallization in different polymer-diluent systems including PVDF with DBP and di(2-ethylhexyl) phthalate (DEHP) [54]. It has also been reported that the secondary crystallization of PVDF could be induced by the entanglement of polymer chains and impingement of spherulites, as well as the perfection of the internal spherulite crystallization [41]. The evidence points to the occurrence of a secondary crystallization of PVDF at a later stage of the crystallization process, which can be ascribed to the enhanced PVDF-diluent interaction along with the addition of TEP (from T0 to T5 and T10). With further addition of F127, the possible weakening of the PVDF-diluent interaction might result in the restoration of the high melting endotherm. In this study, the crystallinity of membranes followed the same tendency with the variation of high melting endotherms as shown in

Table 7. This indicates that the variation of the amorphous portion in PVDF can be controlled by the addition of TEP and F127, which are considered as the N-TIPS inducers in this study. Besides, it can also be noticed that the peak melting temperatures shadowed the similar down-up trend in Fig. 8 (b). The peak melting temperature has been suggested to be related with the degree of the long-range

order in the crystalline structure, which normally has a positive correlation with the crystal size [39, 67, 68]. The results of crystal sizes summarized in

Table 7 conform well to the previous findings and the morphology variations discussed in Section 3.2.

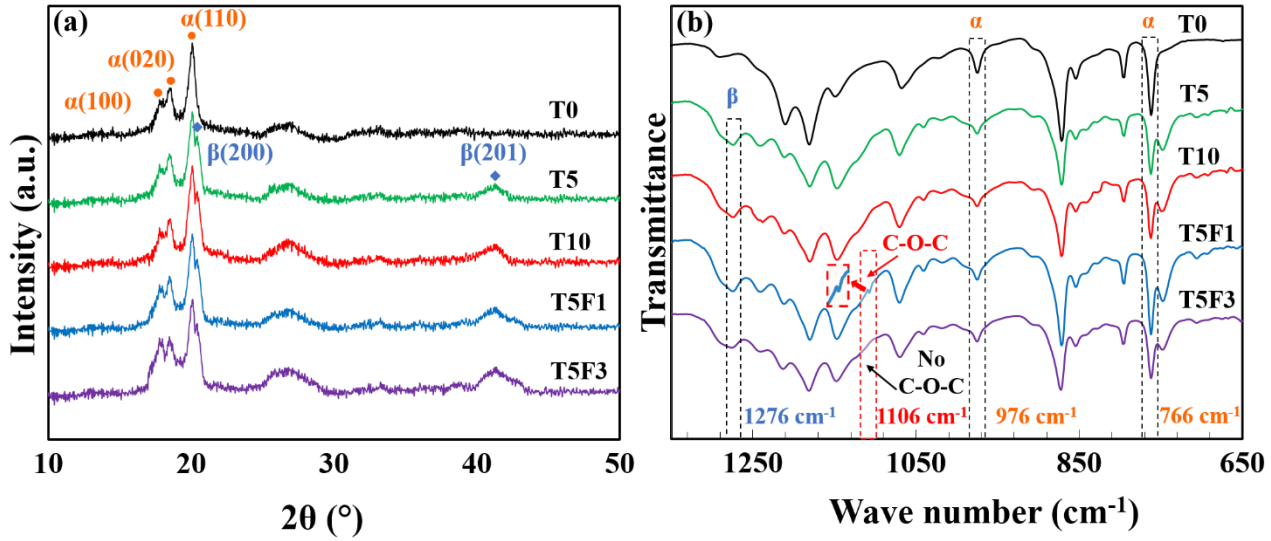

Fig. 9. X-ray diffraction patterns (a) and ATR-FTIR spectra (b) of membranes obtained with different mixed diluents and Pluronic F127 fractions

Table 7. Crystalline properties of membranes obtained with different TEP and Pluronic F127 fractions

Membrane code	ΔH_m (J g^{-1})	χ (%)	D (nm)
T0	51.6 ± 2.1	49.4 ± 2.0	6.33 ± 0.24
T5	50.1 ± 3.3	47.9 ± 3.2	6.01 ± 0.19
T10	46.2 ± 1.9	44.2 ± 2.3	5.71 ± 0.16
T5F1	49.0 ± 2.0	46.9 ± 1.9	6.09 ± 0.12
T5F3	48.5 ± 1.1	46.4 ± 1.6	6.11 ± 0.20

ATR-FTIR analysis was conducted to further investigate the variation of crystalline phases and the presence of F127 in the membrane matrix. Fig. 9(b) depicts the ATR-FTIR spectra for as-spun hollow fiber membranes with different mixed diluents and F127 weight fractions. The presence of peaks at 766 and 976 cm^{-1} confirms the existence of the α-phase for all membranes, while the β-phase was found in the matrix of all TEP-added membranes (T5, T10, T5F1 and T5F3) except for the virgin ones (T0) as suggested by the peaks at 1276 cm^{-1} [3]. This result accords with the findings from WAXD analysis, which implies that the addition of TEP could have a strong effect on the crystallization of PVDF during the membrane formation process.

With regard to F127, it is necessary to validate its presence in the resultant PVDF matrix since F127 is soluble in both the nonsolvent (water) and solvents for the post-treatment (n-hexane and ethanol). It can be seen that the peak at 1106 cm^{-1} only presents in the spectrum of the membranes with 1 wt% addition of F127 (T5F1). The absorbance peak around 1105 to 1115 cm^{-1} normally represents the characteristic band for the C-O-C stretching related to the ether group, which indicates the presence of F127 in the PVDF matrix. It has been found that an anchorage can be provided by the PPO block in F127 molecules, which is likely to help immobilize F127 particles in the PVDF against the elution [69]. However, the absence of the C-O-C peak in the spectrum of membranes with 3 wt% of F127 (T5F3) suggests that a major amount of F127 particles was eluted by either the nonsolvent solvents when the dosing concentration was high. The instability of F127 in the PVDF matrix has also been reported by Loh and co-workers [33, 40, 60]. This phenomenon could be ascribed to the aggregation behaviors of F127 at a high concentration, which possibly turn the F127 particles into spheres in larger sizes and diminish the surface contact of F127 with PVDF [56]. As a result, it became easier for the nonsolvent or solvents to wash out the F127 particles. This is in accord with the variations of contact angle as discussed previously.

3.6 Mechanical properties of hollow fiber membranes

The effect of mixed diluents and F127 addition on the tensile strength and elongation at break is presented in Fig. 10. The sequence of tensile strength is T10 ≈ T5 > T5F1 > T5F3 > T0, while the ranking of elongation is listed as follows: T10 > T5F3 > T5F1 > T5 > T0. In the structure of a semi-crystalline polymer-based membrane, the lamellae crystallites with orderly polymer alignment are embedded between amorphous regions. When spherulites exist in the PVDF-based membranes, the toughness is primarily provided by the intermolecular interactions within the crystallites, while the elasticity is reliant more on the amorphous regions between the lamellae [67]. The former was found to be affected by the polymer-diluent interaction in this study, while the latter can be suggested from the crystallinity as shown in

Table 7. Summarizing the previous results, the strength of polymer-diluent interaction might follow the sequence: T10 > T5 > T5F1 > T5F3 > T0. The ranking of crystallinity is placed as follows: T10 < T5F3 < T5F1 < T5 < T0. By and large, the data conform with this trend with a few exceptions. T10 exhibited lower toughness but higher ductility as compared to T5. This could be attributed to the decreased size of spherulites, which was likely to contain crystalline structure with shorter PVDF chains. Above all, the inducing of N-TIPS effect by addition of TEP and F127 did not weaken the mechanical properties. Instead, the membranes were slightly reinforced as a result of the enhancement in polymer-diluent interaction, showing a tensile strength which ranges from 5.6 ± 0.1 to 6.5 ± 0.2 MPa.

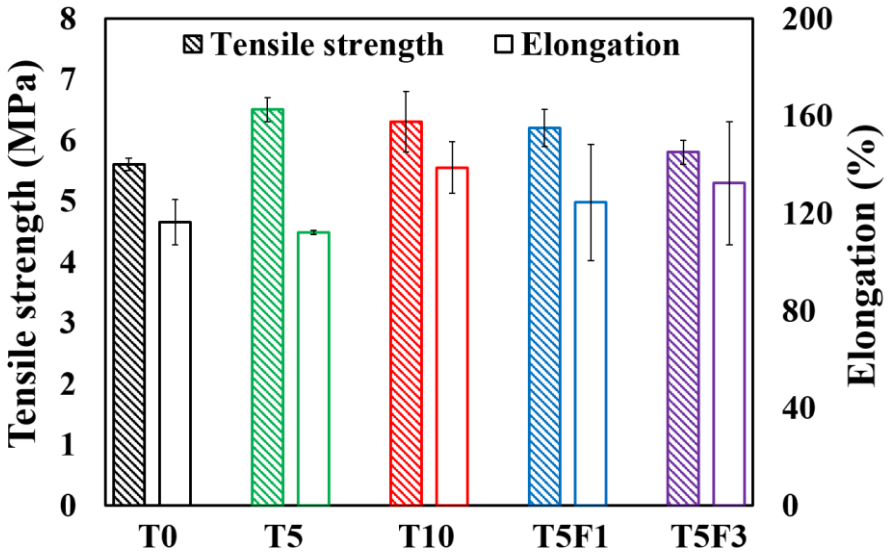

Fig. 10. Mechanical properties of PVDF hollow fiber membranes obtained with different mixed diluents and Pluronic F127 fractions

3.7 Potential applications of prepared hollow fiber membranes

This work has demonstrated that the use of mixed diluents could help induce the occurrence of N-TIPS process, and consequently alter the membrane properties in three major aspects: membrane pore structure, surface roughness and hydrophobicity, as well as polymorphism of PVDF crystals. To further understand the distinct effect of N-TIPS on membrane properties, various PVDF hollow fiber membranes fabricated via NIPS and TIPS are listed together with the T5F1 and T5F3 membranes as shown in Table 8. It can be seen that membranes developed by the N-TIPS method possess improved porosity and water permeability than TIPS membranes without significantly enlarged pore sizes. It is worth noting that the drawback of dense gel layer formation induced by high-concentration TEP, which results in nearly no flux, can be circumvented by using the mixed diluent. Meanwhile, the N-TIPS

membranes have much higher mechanical strength than those prepared via the NIPS method, reaching a level comparable to the TIPS membranes. In addition, the outer surface of prepared N-TIPS membranes are considered relatively hydrophobic due to the intrinsic hydrophobic nature of PVDF and increased roughness contributed by exposed lotus-like spherulitic structure. Such features indicate that the N-TIPS membranes can be used for applications of (1) membrane distillation (requiring hydrophobicity) with further constrained pore size (below 0.1 μm), or (2) microfiltration (requiring hydrophilicity) with further hydrophilic modified outer surface. Besides, the formation of piezoelectric β-phase crystal of PVDF in N-TIPS membranes suggests their potential roles as antifouling piezoelectric membranes or polymer electrolytes for lithium-ion batteries [66].

Table 8. Comparison of various PVDF hollow fiber membranes prepared via phase inversion method

Solvent (diluent)	Method	Tensile stress (MPa)	Mean pore size (μm)	Overall porosity (%)	PWP ($Lm^{-2}h^{-1}bar^{-1}$)	Ref.
DMAc	NIPS	2.5	-[b]	-[b]	116	[70]
DMAc	NIPS	~1.2[a]	-[b]	~90[a]	~190[a]	[71]
DMF*	NIPS	-[b]	0.15	75	-[b]	[72]
NMP	NIPS	3.3	-[b]	74	974	[73]
DEP	TIPS	~4.0[a]	-[b]	-[b]	~500[a]	[74]
DMP	TIPS	9.3[a]	0.12[a]	~65[a]	~71[a]	[58]
GTA	TIPS	~1.5[a]	~0.02[c]	-[b]	767	[75]
TEP	TIPS	6.3	~0.05	~41	0[d]	[55]
ATBC	TIPS	2.2	0.18	61	740	[9]
ATBC	TIPS	~3.4[a]	0.22	~73[a]	~1000[a]	[76]
DMP/TEP (T5F1)	N-TIPS	6.2	0.18	69	922	This work
DMP/TEP (T5F3)	N-TIPS	5.8	0.20	70	1060	This work

Notes:
*Abbreviation: DMF, N,N-Dimethylformamide.
[a)] The data were collected from figures in the literature by using the Digitizer function in *Origin* 9.1.
[b)] The data were not shown in the paper.
[c)] The data were obtained based on the particle rejection (20 nm, > 90%)

[d)] The membrane did show any flux probably due to the formation of dense skin layer [55].

4. Conclusions

In this study, PVDF hollow fiber membranes were developed via a modified N-TIPS method using TEP as a second diluent and Pluronic F127 particles as additives. The bulk morphology of membranes was found to be mainly affected by the polymer-diluent interaction in the TIPS process. The addition of TEP and F127 could jointly initiate the occurrence of the NIPS process at the outer surface before the solidification of membrane structure. Furthermore, the existence of TEP also helped establish a concentration difference on the two sides of inner interface, providing more control over the pore formation. The addition of TEP at 5 wt% was found to be effective in enhancing the polymer-diluent mixture interaction as well as the mutual affinity between the diluent mixture and nonsolvent. The F127 particles were demonstrated to mainly contribute to the pore formation. Consequently, this approach exhibited promising versatility in tailoring the surface pore structure of PVDF hollow fiber membranes without formation of mechanically weak macrovoids. The prepared membranes possess a narrow pore size distribution with enhanced surface and overall porosity. The pure water permeability was correspondingly improved from 389 to above 900 L $m^{-2}h^{-1}bar^{-1}$ with a mean pore size of 0.18 μm. The tensile strength of membranes was well-maintained, ranging from 5.6 ± 0.1 to 6.5 ± 0.2 MPa. Furthermore, the addition of TEP as N-TIPS inducer was found to be correlated to the formation of piezoelectric β-phase crystals of PVDF. Upon specific modification, the preparing PVDF hollow fiber membranes have potential for a wide range of applications, which includes but are not limited to membrane distillation, microfiltration as well as electrochemical-related processes.

Acknowledgments

We acknowledge funding support from the Singapore Economic Development Board to the Singapore Membrane Technology Centre. Special thanks are due to Dr. Loh Chun Heng, Dr. Shanshan Zhao, Dr. Chang Liu and Dr. Yuqing Lin for their valuable suggestions and help.

References

[1] W. Fang, R. Wang, S. Chou, L. Setiawan, A.G. Fane, Composite forward osmosis hollow fiber membranes: Integration of RO- and NF-like selective layers to enhance membrane properties of anti-scaling and anti-internal concentration polarization, J Membr Sci, 394-395 (2012) 140-150.
[2] X.Q. Cheng, Z.X. Wang, X. Jiang, T. Li, C.H. Lau, Z. Guo, J. Ma, L. Shao, Towards sustainable ultrafast molecular-separation membranes: From conventional polymers to emerging materials, Progress in Materials Science, 92 (2018) 258-283.
[3] Z. Cui, E. Drioli, Y.M. Lee, Recent progress in fluoropolymers for membranes, Progress in Polymer Science, 39 (2014) 164-198.
[4] M.J. Mulder, Basic principles of membrane technology, Kluwer Academic Publishers, 1996.
[5] J.T. Jung, J.F. Kim, H.H. Wang, E. di Nicolo, E. Drioli, Y.M. Lee, Understanding the non-solvent induced phase separation (NIPS) effect during the fabrication of microporous PVDF membranes via thermally induced phase separation (TIPS), J Membr Sci, 514 (2016) 250-263.
[6] S. Rajabzadeh, T. Maruyama, Y. Ohmukai, T. Sotani, H. Matsuyama, Preparation of PVDF/PMMA blend hollow fiber membrane via thermally induced phase separation (TIPS) method, Separation and Purification Technology, 66 (2009) 76-83.
[7] H. Matsuyama, T. Maki, M. Teramoto, K. Asano, Effect of polypropylene molecular weight on porous membrane formation by thermally induced phase separation, J Membr Sci, 204 (2002) 323-328.
[8] J.F. Kim, J.H. Kim, Y.M. Lee, E. Drioli, Thermally induced phase separation and electrospinning methods for emerging membrane applications: A review, AIChE Journal, 62 (2016) 461-490.
[9] Z. Cui, N.T. Hassankiadeh, S.Y. Lee, J.M. Lee, K.T. Woo, A. Sanguineti, V. Arcella, Y.M. Lee, E. Drioli, Poly(vinylidene fluoride) membrane preparation with an environmental diluent via thermally induced phase separation, J Membr Sci, 444 (2013) 223-236.
[10] L. Shi, R. Wang, Y. Cao, C. Feng, D.T. Liang, J.H. Tay, Fabrication of poly(vinylidene fluoride-co-hexafluropropylene) (PVDF-HFP) asymmetric microporous hollow fiber membranes, J Membr Sci, 305 (2007) 215-225.
[11] J.T. Jung, H.H. Wang, J.F. Kim, J. Lee, J.S. Kim, E. Drioli, Y.M. Lee, Tailoring nonsolvent-thermally induced phase separation (N-TIPS) effect using triple spinneret to fabricate high performance PVDF hollow fiber membranes, J Membr Sci, 559 (2018) 117-126.
[12] P. van de Witte, P.J. Dijkstra, J.W.A. van den Berg, J. Feijen, Phase separation processes in polymer solutions in relation to membrane formation, J Membr Sci, 117 (1996) 1-31.
[13] S. Wongchitphimon, R. Wang, R. Jiraratananon, L. Shi, C.H. Loh, Effect of polyethylene glycol (PEG) as an additive on the fabrication of polyvinylidene fluoride-co-hexafluropropylene (PVDF-HFP) asymmetric microporous hollow fiber membranes, J Membr Sci, 369 (2011) 329-338.
[14] L. Shi, R. Wang, Y. Cao, D.T. Liang, J.H. Tay, Effect of additives on the fabrication of poly(vinylidene fluoride-co-hexafluropropylene) (PVDF-HFP) asymmetric microporous hollow fiber membranes, J Membr Sci, 315 (2008) 195-204.
[15] H. Matsuyama, Y. Takida, T. Maki, M. Teramoto, Preparation of porous membrane by combined use of thermally induced phase separation and immersion precipitation, Polymer, 43 (2002) 5243-5248.
[16] F. Liu, N.A. Hashim, Y. Liu, M.R.M. Abed, K. Li, Progress in the production and modification of PVDF membranes, J Membr Sci, 375 (2011) 1-27.
[17] F. Liu, M.-m. Tao, L.-x. Xue, PVDF membranes with inter-connected pores prepared via a Nat-ips process, Desalination, 298 (2012) 99-105.
[18] L. Wu, J. Sun, An improved process for polyvinylidene fluoride membrane preparation by using a water soluble diluent via thermally induced phase separation technique, Materials & Design, 86 (2015) 204-214.

[19] N.T. Hassankiadeh, Z. Cui, J.H. Kim, D.W. Shin, S.Y. Lee, A. Sanguineti, V. Arcella, Y.M. Lee, E. Drioli, Microporous poly(vinylidene fluoride) hollow fiber membranes fabricated with PolarClean as water-soluble green diluent and additives, J Membr Sci, 479 (2015) 204-212.
[20] T. Xiao, P. Wang, X. Yang, X. Cai, J. Lu, Fabrication and characterization of novel asymmetric polyvinylidene fluoride (PVDF) membranes by the nonsolvent thermally induced phase separation (NTIPS) method for membrane distillation applications, J Membr Sci, 489 (2015) 160-174.
[21] L. Wu, J. Sun, Structure and properties of PVDF membrane with PES-C addition via thermally induced phase separation process, Applied Surface Science, 322 (2014) 101-110.
[22] X. Li, Y. Wang, X. Lu, C. Xiao, Morphology changes of polyvinylidene fluoride membrane under different phase separation mechanisms, J Membr Sci, 320 (2008) 477-482.
[23] H.-P. Xu, W.-Z. Lang, X. Zhang, Y.-J. Guo, Preparation and characterizations of charged PVDF membranes via composite thermally induced phase separation(c-TIPS) method, Journal of Industrial and Engineering Chemistry, (2015).
[24] A.W. Qin, X. Li, B.M. Ma, C.Y. Liu, X.Z. Zhao, C.J. He, Preparation and characterization of poly (vinylidene fluoride) hollow fiber membranes via modified thermally induced phase separation process, Advanced Materials Research, 734-737 (2013) 2172-2175.
[25] J. Liu, X. Lu, J. Li, C. Wu, Preparation and properties of poly (vinylidene fluoride) membranes via the low temperature thermally induced phase separation method, Journal of Polymer Research, 21 (2014) 1-16.
[26] D.R. Lloyd, K.E. Kinzer, H.S. Tseng, Microporous membrane formation via thermally induced phase separation. I. Solid-liquid phase separation, J Membr Sci, 52 (1990) 239-261.
[27] J. Lee, B. Park, J. Kim, S.B. Park, Effect of PVP, lithium chloride, and glycerol additives on PVDF dual-layer hollow fiber membranes fabricated using simultaneous spinning of TIPS and NIPS, Macromolecular Research, 23 (2015) 291-299.
[28] C. Fang, S. Jeon, S. Rajabzadeh, L. Cheng, L. Fang, H. Matsuyama, Tailoring the surface pore size of hollow fiber membranes in the TIPS process, Journal of Materials Chemistry A, 6 (2018) 535-547.
[29] L. Setiawan, L. Shi, W.B. Krantz, R. Wang, Explorations of delamination and irregular structure in poly(amide-imide)-polyethersulfone dual layer hollow fiber membranes, J Membr Sci, 423–424 (2012) 73-84.
[30] L. Shi, R. Wang, Y. Cao, Effect of the rheology of poly(vinylidene fluoride-co-hexafluropropylene) (PVDF-HFP) dope solutions on the formation of microporous hollow fibers used as membrane contactors, J Membr Sci, 344 (2009) 112-122.
[31] R. Wang, L. Shi, C.Y. Tang, S. Chou, C. Qiu, A.G. Fane, Characterization of novel forward osmosis hollow fiber membranes, J Membr Sci, 355 (2010) 158-167.
[32] S. Chou, L. Shi, R. Wang, C.Y. Tang, C. Qiu, A.G. Fane, Characteristics and potential applications of a novel forward osmosis hollow fiber membrane, Desalination, 261 (2010) 365-372.
[33] C.H. Loh, R. Wang, L. Shi, A.G. Fane, Fabrication of high performance polyethersulfone UF hollow fiber membranes using amphiphilic pluronic block copolymers as pore-forming additives, J Membr Sci, 380 (2011) 114-123.
[34] A. Bottino, G. Camera-Roda, G. Capannelli, S. Munari, The formation of microporous polyvinylidene difluoride membranes by phase separation, J Membr Sci, 57 (1991) 1-20.
[35] D.-J. Lin, H.-H. Chang, T.-C. Chen, Y.-C. Lee, L.-P. Cheng, Formation of porous poly(vinylidene fluoride) membranes with symmetric or asymmetric morphology by immersion precipitation in the water/TEP/PVDF system, European Polymer Journal, 42 (2006) 1581-1594.
[36] A. Figoli, T. Marino, S. Simone, E. Di Nicolò, X.M. Li, T. He, S. Tornaghi, E. Drioli, Towards non-toxic solvents for membrane preparation: A review, Green Chemistry, 16 (2014) 4034-4059.
[37] T. Marino, S. Blefari, E. Di Nicolò, A. Figoli, A more sustainable membrane preparation using triethyl phosphate as solvent, in: Green Processing and Synthesis, 2017, pp. 295.

[38] T. Marino, F. Russo, A. Figoli, The formation of polyvinylidene fluoride membranes with tailored properties via vapour/non-solvent induced phase separation, Membranes, 8 (2018) 71.
[39] J. Zhao, L. Shi, C.H. Loh, R. Wang, Preparation of PVDF/PTFE hollow fiber membranes for direct contact membrane distillation via thermally induced phase separation method, Desalination, 430 (2018) 86-97.
[40] C. Loh, R. Wang, Fabrication of PVDF hollow fiber membranes: Effects of low-concentration pluronic and spinning conditions, J Membr Sci, 466 (2014) 130-141.
[41] G.-L. Ji, B.-K. Zhu, Z.-Y. Cui, C.-F. Zhang, Y.-Y. Xu, PVDF porous matrix with controlled microstructure prepared by TIPS process as polymer electrolyte for lithium ion battery, Polymer, 48 (2007) 6415-6425.
[42] Z. Zhang, C. Guo, X. Li, G. Liu, J. Lv, Effects of PVDF Crystallization on Polymer Gelation Behavior and Membrane Structure from PVDF/TEP System via Modified TIPS Process, Polymer-Plastics Technology and Engineering, 52 (2013) 564-570.
[43] T. Ma, Z. Cui, Y. Wu, S. Qin, H. Wang, F. Yan, N. Han, J. Li, Preparation of PVDF based blend microporous membranes for lithium ion batteries by thermally induced phase separation: I. Effect of PMMA on the membrane formation process and the properties, J Membr Sci, 444 (2013) 213-222.
[44] Solvay, Solef 6020 PVDF Technical Data Sheet, in, 2014.
[45] G. Chen, X. Yang, Y. Lu, R. Wang, A.G. Fane, Heat transfer intensification and scaling mitigation in bubbling-enhanced membrane distillation for brine concentration, J Membr Sci, 470 (2014) 60-69.
[46] A.L. Patterson, The Scherrer Formula for X-Ray Particle Size Determination, Physical Review, 56 (1939) 978-982.
[47] A.W. Burton, K. Ong, T. Rea, I.Y. Chan, On the estimation of average crystallite size of zeolites from the Scherrer equation: A critical evaluation of its application to zeolites with one-dimensional pore systems, Micropor Mesopor Mat, 117 (2009) 75-90.
[48] L. Setiawan, R. Wang, L. Shi, K. Li, A.G. Fane, Novel dual-layer hollow fiber membranes applied for forward osmosis process, J Membr Sci, 421-422 (2012) 238-246.
[49] C.M. Hansen, Hansen solubility parameters: a user's handbook, CRC press, 2012.
[50] J. Yang, X.L. Wang, F. Tian, Y.K. Lin, Z. Wang, Diluent selection of PVDF membrane prepared via thermally induced phase separation, Gaodeng Xuexiao Huaxue Xuebao/Chemical Journal of Chinese Universities, 29 (2008) 1895-1900.
[51] J.R. Fried, Conformations, solutions and molecular weight, in: Polymer Science and Technology, Prentice Hall Professional Technical Reference, 2003.
[52] T. Lindvig, M.L. Michelsen, G.M. Kontogeorgis, A flory–huggins model based on the hansen solubility parameters, Fluid phase equilibria, 203 (2002) 247-260.
[53] B. Liu, Q. Du, Y. Yang, The phase diagrams of mixtures of EVAL and PEG in relation to membrane formation, J Membr Sci, 180 (2000) 81-92.
[54] G.L. Ji, L.P. Zhu, B.K. Zhu, Y.Y. Xu, Effect of diluents on crystallization of poly(vinylidene fluoride) and phase separated structure in a ternary system via thermally induced phase separation, Chinese Journal of Polymer Science (English Edition), 26 (2008) 291-298.
[55] Z. Zhang, C. Guo, G. Liu, X. Li, Y. Guan, J. Lv, Effect of TEP content in cooling bath on porous structure, crystalline and mechanical properties of PVDF hollow fiber membranes, Polymer Engineering & Science, 54 (2014) 2207-2214.
[56] M. Vasilescu, R. Bandula, Aggregation of Pluronic F127 and polydimethylsiloxane-graft-polyether block copolymers in water and microstructure of aggregates as evaluated by molecular probe techniques, Rev Roum Chim, 56 (2011) 57-64.
[57] X.Y. Xiong, K.C. Tam, L.H. Gan, Synthesis and Aggregation Behavior of Pluronic F127/Poly(lactic acid) Block Copolymers in Aqueous Solutions, Macromolecules, 36 (2003) 9979-9985.
[58] F. Shi, Y. Ma, J. Ma, P. Wang, W. Sun, Preparation and characterization of PVDF/TiO2 hybrid membranes with different dosage of nano-TiO2, J Membr Sci, 389 (2012) 522-531.

[59] W. Zhao, Y. Su, C. Li, Q. Shi, X. Ning, Z. Jiang, Fabrication of antifouling polyethersulfone ultrafiltration membranes using Pluronic F127 as both surface modifier and pore-forming agent, J Membr Sci, 318 (2008) 405-412.
[60] C.H. Loh, R. Wang, Effects of additives and coagulant temperature on fabrication of high performance PVDF/pluronic F127 blend hollow fiber membranes via nonsolvent induced phase separation, Chinese Journal of Chemical Engineering, 20 (2012) 71-79.
[61] C.H. Loh, R. Wang, Insight into the role of amphiphilic pluronic block copolymer as pore-forming additive in PVDF membrane formation, J Membr Sci, 446 (2013) 492-503.
[62] R. F., Secondary crystallization of polymers, Journal of Polymer Science, 44 (1960) 517-522.
[63] D. Chun‐Hui, W. Chun‐Jin, W. Li‐Guang, Effects of pluronic F127 on the polymorphism and thermoresponsive properties of PVDF blend membranes via immersion precipitation process, J Appl Polym Sci, 124 (2012) E330-E337.
[64] M.-m. Tao, F. Liu, B.-r. Ma, L.-x. Xue, Effect of solvent power on PVDF membrane polymorphism during phase inversion, Desalination, 316 (2013) 137-145.
[65] M. Zhang, A.-Q. Zhang, B.-K. Zhu, C.-H. Du, Y.-Y. Xu, Polymorphism in porous poly(vinylidene fluoride) membranes formed via immersion precipitation process, J Membr Sci, 319 (2008) 169-175.
[66] Z. Cui, N.T. Hassankiadeh, Y. Zhuang, E. Drioli, Y.M. Lee, Crystalline polymorphism in poly(vinylidenefluoride) membranes, Progress in Polymer Science, 51 (2015) 94-126.
[67] G.W. Ehrenstein, Polymeric Materials: Structure, Properties, Applications, Carl Hanser Verlag GmbH & Company KG, 2012.
[68] M. Raimo, Estimation of polymer nucleation and growth rates by overall DSC crystallization rates, Polymer Journal, 43 (2011) 78.
[69] Y.-q. Wang, T. Wang, Y.-l. Su, F.-b. Peng, H. Wu, Z.-y. Jiang, Remarkable Reduction of Irreversible Fouling and Improvement of the Permeation Properties of Poly(ether sulfone) Ultrafiltration Membranes by Blending with Pluronic F127, Langmuir, 21 (2005) 11856-11862.
[70] M.R. Moghareh Abed, S.C. Kumbharkar, A.M. Groth, K. Li, Economical production of PVDF-g-POEM for use as a blend in preparation of PVDF based hydrophilic hollow fibre membranes, Separation and Purification Technology, 106 (2013) 47-55.
[71] Y. Zhang, R. Lin, M. Yuan, X. Yue, Effects of pore-forming additives on structures and properties of PVDF/Fe3+/Cu2+ hollow fiber membranes, Desalination and Water Treatment, 51 (2013) 3903-3908.
[72] S. Simone, A. Figoli, A. Criscuoli, M.C. Carnevale, A. Rosselli, E. Drioli, Preparation of hollow fibre membranes from PVDF/PVP blends and their application in VMD, J Membr Sci, 364 (2010) 219-232.
[73] F. Zhang, W. Zhang, Y. Yu, B. Deng, J. Li, J. Jin, Sol–gel preparation of PAA-g-PVDF/TiO2 nanocomposite hollow fiber membranes with extremely high water flux and improved antifouling property, J Membr Sci, 432 (2013) 25-32.
[74] S. Rajabzadeh, C. Liang, Y. Ohmukai, T. Maruyama, H. Matsuyama, Effect of additives on the morphology and properties of poly(vinylidene fluoride) blend hollow fiber membrane prepared by the thermally induced phase separation method, J Membr Sci, 423–424 (2012) 189-194.
[75] S. Rajabzadeh, T. Maruyama, T. Sotani, H. Matsuyama, Preparation of PVDF hollow fiber membrane from a ternary polymer/solvent/nonsolvent system via thermally induced phase separation (TIPS) method, Separation and Purification Technology, 63 (2008) 415-423.
[76] N.T. Hassankiadeh, Z. Cui, J.H. Kim, D.W. Shin, A. Sanguineti, V. Arcella, Y.M. Lee, E. Drioli, PVDF hollow fiber membranes prepared from green diluent via thermally induced phase separation: Effect of PVDF molecular weight, J Membr Sci, 471 (2014) 237-246.